molecular pharmaceutics

Article

A Potent Acetylcholinesterase Selective and Reversible Homodimeric Agent based on Tacrine for Theranostics

Virendra Kumar Meena, Shubhra Chaturvedi, Rakesh Kumar Sharma, Anil Kumar Mishra, and Puja Panwar Hazari

Mol. Pharmaceutics, **Just Accepted Manuscript** • DOI: 10.1021/acs.molpharmaceut.8b01058 • Publication Date (Web): 06 May 2019

ACS Publications

is published by the American Chemical Society. 1155 Sixteenth Street N.W., Washington, DC 20036

A Potent Acetylcholinesterase Selective and Reversible Homodimeric Agent based on Tacrine for Theranostics

Virendra Kumar Meena[a,b], *ShubhraChaturvedi*[a], *Rakesh Kumar Sharma*[b], *Anil Kumar Mishra*[a], *Puja Panwar Hazari*[a,*]

[a]Division of Cyclotron and Radiopharmaceutical Sciences, Institute of Nuclear Medicine and Allied Sciences, Brig S.K. Mazumdar Road, Delhi-110054, India.

[b]Department of Chemistry, University of Delhi, Delhi-110007, India

*Corresponding author

Dr. Puja PanwarHazari

Brig. S. K. Mazumdar Road, Delhi-110054, India

Phone: +91-11-23984480 Fax: +91-11-2391-9509

E-mail: puja.hazari@gmail.com

KEYWORDS: Alzheimer's disease, Acetylcholinesterase, Tacrine, Multi-target directed ligands, Amyloid β peptide, Theranostic Agent

Abstract

Acetylcholinesterase (AChE) has been an important biomarker for diagnosing Alzheimer's disease (AD), due to reduction in AChE activity in postmortem brains of AD patients. A potent, selective and reversible homodimeric inhibitor of acetylcholinesterase (AChE), 5-amino-N^1,N^3-bis(2-(1,2,3,4-tetrahydroacridin-9-ylamino)ethyl)isophthalamide [Compound **(4)**] was synthesized by using 9-alkyl(1,2,3,4-tetrahydroacridine) pharmacophore with appended functionality. In the present work, we report the synthesis of this bivalent inhibitor of AChE.The homodimeric ligand structure was designed and studied with molecular docking tools which revealed its high affinity and interactions with active site gorge of AChE which includes both catalytic active site (CAS) and peripheral active site (PAS).The IC_{50} value of this bivalent inhibitor for AChE and BuChE were 0.54 ± 0.06 and 32.49 ± 1.2 nM respectively, with a selectivity ratio of 60.16 towards AChE. The designed ligand also showed potent inhibitory properties on PAS activity as well as on AChE-induced amyloid aggregation with low cytotoxicity on rat hippocampal neurons. The AFM images further corroborated the $A\beta_{1-42}$ aggregation inhibition by compound (4) to extent similar like Bis(7)-tacrine. Moreover, the bivalent ligand was also proven to be of neurogenic potential due to its ability to induce S-phase post-treatment in rat hippocampal neuronal cells. On the basis of initial results, the agent could be further explored for its theranostic value clinically, which gives the possibility of tracing the AChE levels by molecular imaging techniques in correlation with progression of neurocognitive disorders like Alzheimer's disease for better therapy response and patient management.

Abbreviations: Alzheimer's disease (AD), Amyloid β Peptide (Aβ), Acetylcholinesterase (AChE), Catalytic active site (CAS), Peripheral active site (PAS), Multi-target directed ligands (MTDL)

Introduction

Alzheimer's disease (AD) is the most common cause of dementia among the elderly people with a multitude of multi-facet pathologies associated with neurodegeneration [1-2]. It is commonly characterized by memory impairment and gradual deficits in various cognitive domains.[3] The neuropathological hallmarks include aggregation of amyloid-beta 1-40/42 (Aβ) peptide inside the soma of the neurons derived from the altered metabolism of APP protein by enzymes such as α- and β-secretases, along with the appearance of neurofibrillary tangles (NFT) due to aggregation of hyper phosphorylated tau proteins.[4-6] Aβ oligomers are implicated in many of the molecular events during neurodegeneration which includes neurotoxicity, dysregulation of Ca^{+2} level homeostasis and chronic activation of microglial cells inside the brain which leads to neuro-inflammation.[7-10] However, many of the causative pathways for this neurodegeneration are still unclear, suggesting its multi-facet nature. Various theories have been forwarded to explain the pathogenesis of Alzheimer's disease including cholinergic hypothesis, the amyloid cascade hypothesis and oxidative stress hypothesis with free radical generation depicting an intertwined situation. There have been a number of diagnostic biomarkers used for detecting AD condition. These biomarkers include neurochemical markers (i.e. Aβ peptides, total tau protein, phosphorylated tau and AChE etc.) and neuroimaging markers (i.e. hippocampal volumetry, entorhinal cortex volumetry etc.). Changes in various biochemical and histopathological neurotransmitter markers results from use of cholinomimetic drugs speculate an association between decline in learning and memory with deficit in excitatory amino acid (EAA) neurotransmission. Therefore, many therapeutic interventions has emerged aiming to restore the loss of cholinergic neurotransmission by inhibiting AChE at cholinergic synapses in AD brain. [11-13]Not surprising, AChE activity was assumed to be one of the major neurochemical biomarker for degeneration of cholinergic neural network. [14]AChE activity can be considered as the major therapeutic target as well as diagnostic biomarker for detecting AD condition. The activity or density of cerebral AChE was thoroughly studied by PET imaging in various tissues in

different disease states.[15-16] Previous studies has shown a decline in AChE activity in cerebral cortex was reported in necropsy brain studies. Therefore, *in vivo* AChE activity measurement could provide useful insight not only in disease diagnosis, monitoring disease progression but also assist in therapeutic outcome of anti-dementia drugs. [17]

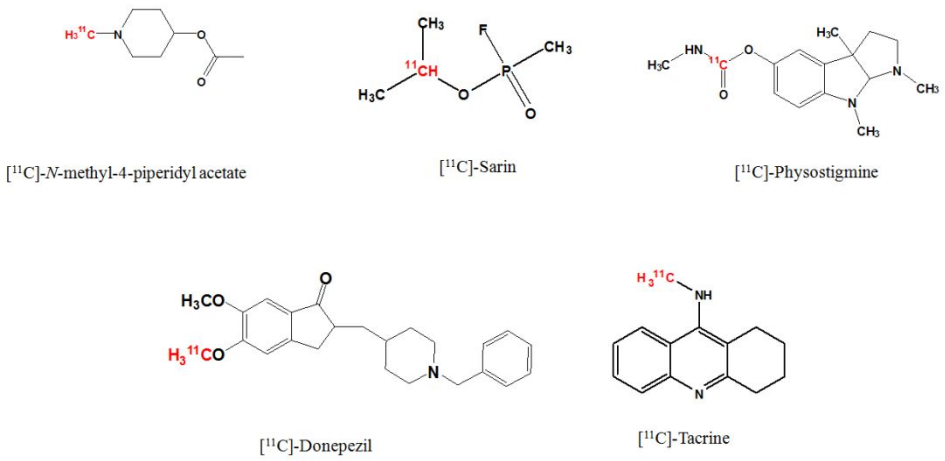

Fig. 1 Different classes of ^{11}C-labeled PET radiotracers for cerebral acetylcholinesterase (AChE).

For studying the distribution pattern of AChE in various regions of brain, PET radiotracers for AChE are available using two radiopharmaceutical approaches. The one uses radiolabeled lipophilic acetylcholine analogs which acts as substrate for cerebral AChE and, second uses radiolabeled AChE inhibitors as radiotracer which are presented in **Fig. 1**. Initially various substrates based radioligands for AChE were developed, such as [^{11}C]-*N*-methyl-4-piperidyl acetate [^{11}C]-MP4A and [^{11}C]-MP4P which are analogs of acetylcholine. [^{11}C]-MP4A, unlike acetylcholine was able to cross blood brain barrier, and further cleaved by AChE into [^{11}C]-*N*-methyl-4-piperidinol, a hydrophilic metabolite which is trapped in the brain due to low blood brain barrier permeability.[18] But the radiolabeled metabolite gave very diffuse radioactivity signal inside the brain and failed to match the histochemical location of AChE inside the AD brain.[19] Another approach uses radiolabeled inhibitors of AChE, i.e. [^{18}F]-CP118 954, [^{11}C]-Sarin, [^{11}C]-Physostigmine, [^{11}C]-Donepezil, [^{11}C]-Tacrine etc., which are reversible inhibitors of

AChE showing excellent brain penetration, show longer retention time, appropriate pharmacokinetics and match the histological location of AChE in AD brain.[20-24]

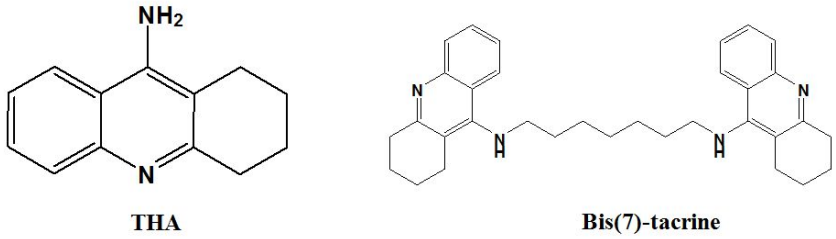

Fig 2. Chemical structures of Tacrine (THA) and Bis(7)-tacrine.

Tacrine (THA) provides a scaffold to design and synthesizeAChE inhibitors with high specificity and potency, which acts as multi-target directed ligands (MTDLs) with anti-Alzheimer properties. [25-27]These ligands show selectivity towards AChE and also inhibit the aggregation of Aβ (1-40/42) peptide *in vitro* and *in vivo*. [28] A wide spectrum of tacrine conjugates were made, but bis-alkyl-tacrines are the most potent inhibitors reported of AChE activity with amyloid aggregation inhibition. The mechanism of action of these bis-tacrine inhibitors via blocking the both active sites of the AChE, CAS (Catalytic active site) which metabolizes the acetylcholine into acetyl and choline at the site of action, and PAS (Peripheral active site) which facilitates the aggregation of Aβ peptides. [29] With inhibition of AChE the levels of acetylcholine increase in cholinergic system to improve the cholinergic neurotransmission as well as cognition function in patients. Therefore, ligands with dual functionality as imaging tracer with therapeutic potential for disorders involving AChE are much needed.

The present work has been directed for development of next generation of ligands which could be used in nanomolar concentrations for probing the enzyme with therapeutic effects in same concentration range. A homodimeric AChE targeted tracer was constructed using THA pharmacophore with aromatic linker which has suitable site for [^{11}C] radiolabeling without affecting the specificity and affinity towards its target. Here, we report the synthesis of new

homodimeric ligand 5-amino-*N*[1],*N*[3]-bis(2-(1,2,3,4-tetrahydroacridin-9-ylamino)ethyl)isophthalamide **(4)** and potential of this ligand as anti-Alzheimer's agent.Therefore, this ligand could be advantageous in critical patient management by monitoring the disease progression and therapeutic outcome.

Chemicals and Reagents

Anthranilic acid, Cyclohexanone, Phosphorous(V) oxychloride, Ethylene diamine, Phenol, 5-Aminoisopthalic acid (5-AIA), 1-hydroxybenzotriazole (HOBt) and 1-ethyl-3-(3-dimethylaminopropyl) carbodiimide hydrochloride (EDC) and Triethylamine (TEA) were purchased from Merck Ltd (India). Reagents and chemicals were commercially purchased and used without further purification unless mentioned. C-18 Sep-pak plus cartridges were procured from Waters Corporation (Milford, MA, 120 USA)

Instrumentation

Thin layer chromatography (TLC) was carried using Merck Silica Gel 60 F_{254}, 20x20 cm plates and viewed under 254nm UV lamp. ^{1}H and ^{13}C NMR spectra were recorded on Bruker AVANCE II 400 MHz NMR system (Ultra-shielded) using solvents D_2O, $CDCl_3$, CD_3OD and DMSO-d_6. Agilent 6310 ion trap mass spectrometer was used for electrospray ionization mass spectroscopy (ESI-MS) in positive and negative ion mode. High resolution mass spectroscopy (QTOF) coupled with liquid chromatography mass spectrometry (HRMS-LCMS) was used to obtain accurate mass of the compounds.

General methods for synthesis

*Scheme 1. 9-Chloro-1,2,3,4-tetrahydroacridine***(1)**. To a mixture of Anthranilic acid (1g, 7.283 mmol) and cyclohexanone (0.724mL, 6.986 mmol) on an ice bath, $POCl_3$ (6.756mL) was carefully and stirred for 15 min. The mixture was then heated under reflux (130^{o}C) for 3 h, and the reaction mixture was cooled to room temperature. The reaction mixture was then added to

10% KOH solution in a beaker on ice bath with stirring. The mixture was further extracted with ethyl acetate. The organic layer was dried over anhydrous sodium sulfate and concentrated *in vacuo*, affording an organish-yellow solid. It was further purified by silica gel chromatography, and eluted with petroleum ether: ethyl acetate (8:2) to give the pale-yellow product. (1.54g, 94%): mp 68-70C; ^{1}H NMR (400MHz, $CDCl_3$, 25ºC) δ (ppm)1.97 (s, 4H, CH_2-CH_2), 3.0 (t, 2H,*J =6.4Hz*, CH_2), 3.1 (t, 2H, CH_2), 7.55 (t, 1H,*J = 8Hz*, ArH), 7.68 (m, 1H, ArH), 8.00 (d, 1H,*J = 8.4Hz*, ArH), 8.17(d, 1H, *J = 8.4Hz*, ArH);^{13}C NMR (400MHz, CDCl3, 25ºC) δ (ppm)22.64, 22.68, 27.52, 34.20, 123.71, 125.40, 126.50, 128.62, 128.89, 129.28, 141.49, 146.66, 159.52; ESI-MS$^+$: m/z calculated for$C_{13}H_{12}$Cl N [M + H]$^+$, 218.69; found [M + H]$^+$, 218.20; HRMS (positive ions): m/z calculated for [M + H]$^+$ 218.6941; found [M + H]$^+$, 218.0734.

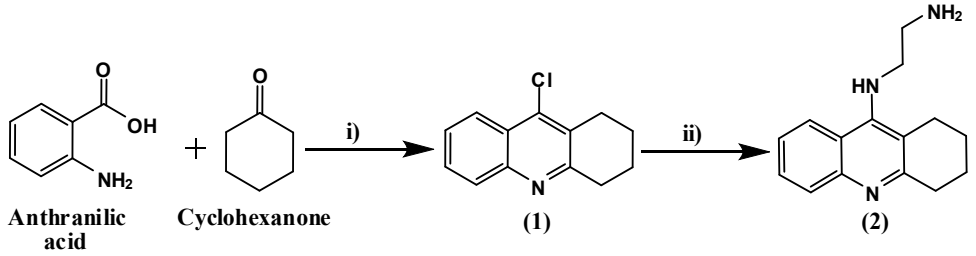

Scheme 1. Synthesis of N^1-(1,2,3,4-tetrahydroacridin-9-yl)ethane-1,2-diamine (2). Reagents and conditions: i) $POCl_3$, Reflux, 3h; ii) $NH_2(CH_2)_2NH_2$, Phenol, NaI, 180˚C, 3h.

N^1-(1,2,3,4-tetrahydroacridin-9-yl)ethane-1,2-diamine **(2)**. To the mixture of intermediate **(1)** (0.50g, 2.296mmol), phenol (1.0g), ethylenediamine (5.0mL, 65.90mmol) and NaI (0.05g) was carefully added and heated to 180°C under inert nitrogen conditions for 3 h. The mixture was then cooled to room temperature and diluted with dichloromethane, then this mixture was made basic with 10% KOH solution. The organic layer was washed with water and brine, and dried over anhydrous sodium sulfate. The residue was further purified with silica gel chromatography, and eluted with dichloromethane: methanol (9.0:1.0) with 7mL (aq. NH_3, 30%) per liter of solution to give product as pale yellow solid. (0.48g, 88%); ^{1}H NMR (400MHz, CD_3OD, 25ºC) δ (ppm) 1.98-2.00 (t, 4H, CH_2-CH_2), 2.8 (s, 2H, CH_2), 3.0 (s, 2H, CH_2), 3.4 (t, 2H, CH_2), 4.2 (t,

2H,*J* = *6.4Hz*, CH_2), 7.6 (t, 1H,*J* = *8Hz*, ArH), 7.8 (d, 1H,*J* = *8Hz*, ArH), 7.8 (d, 1H, ArH), 8.3(d, 1H,*J* = *10Hz*, ArH);^{13}C NMR (400MHz, CD_3OD, 25ºC) δ (ppm) 20.29, 21.52, 23.73, 27.99, 38.97, 44.61, 112.66, 115.94, 118.95, 124.54, 125.49, 132.82, 138.24, 151.33, 156.72; ESI-MS$^+$: m/z calculated for$C_{15}H_{19}N_3$ $[M + H]^+$, 242.33; found $[M + H]^+$, 242.20; HRMS (positive ions): m/z calculated for $[M + H]^+$ 242.3315; found $[M + H]^+$, 242.1654

*Scheme 2. 5-amino-N^1,N^3-bis(2-(1,2,3,4-tetrahydroacridin-9-ylamino)ethyl)isophthalamide***(4)**.
To a solution of 5-Aminoisophthalic acid (100mg, 0.552 mmol) in 10 mL anhydrous DMF with N_2 supply on ice bath were added 1-hydroxybenzotriazole (HOBt,) (164 mg, 1.2144 mmol) and 1-ethyl-3-(3-dimethylaminopropyl) carbodiimide hydrochloride (EDC,) (232.8 mg, 1.2144 mmol) and kept on stirring for another 15 min. The amine intermediate **(2)**(293.1 mg, 1.2144mmol) was added in a dropwise manner to the above resulting solution on ice bath. The mixture solution was allowed to stir for another 30 min and trimethylamine (TEA) was added with continued stirring overnight (12h-18h). Next day, the mixture was evaporated in vacuo and the residue was washed twice with mixture of DCM with water. The organic fraction was again washed with saturated brine to yield the final product. The DCM was dried in vacuo to afford the final product **(4)** in form as pale white solid. This residue was further purified by silica gel column chromatography, and eluted with mixture of dichloromethane: methanol (8:2) with 7mL (aq. NH3, 30% solution) per liter of the mixture to give product as white solid. (230 mg, 30.2%), ^{1}H NMR (400MHz, CD_3OD, 25ºC) δ (ppm)1.9 (m, 8H, 2 X CH_2-CH_2), 2.8 (s, 4H, 2 X CH_2), 3.0 (s, 4H, 2 X CH_2), 3.6 (t, 4H, 2 X CH_2), 3.7 (t, 4H,*J* = *5.6Hz*, 2 X CH_2), 7.3 (t, 2H, *J* = *8Hz*, 2 X ArH), 7.6 (t, 2H,*J* = *8Hz*, 2 X ArH), 7.8 (d, 2H, 2 X ArH), 8.1 (d, 2H,*J* = *8Hz*, 2 X ArH);^{13}C NMR (400MHz, CD_3OD, 25ºC) δ (ppm) 22.34, 22.68, 24.43, 32.91, 50.46, 61.12, 116.27, 120.21, 123.07, 123.47, 126.73, 128.30, 146.69, 151.81, 157.98, 160.05; ESI-MS$^+$: m/z calculated for$C_{15}H_{19}N_3$ $[M + H]^+$, 628.78; found $[M + H]^+$, 628.6; $[M/2Z + H]^+$, 314.8; HRMS (positive ions): m/z calculated for $[M + H]^+$ 627.7778; found $[M + H]^+$, 628.3380; $[M/2Z + H]^+$, 314.6727.

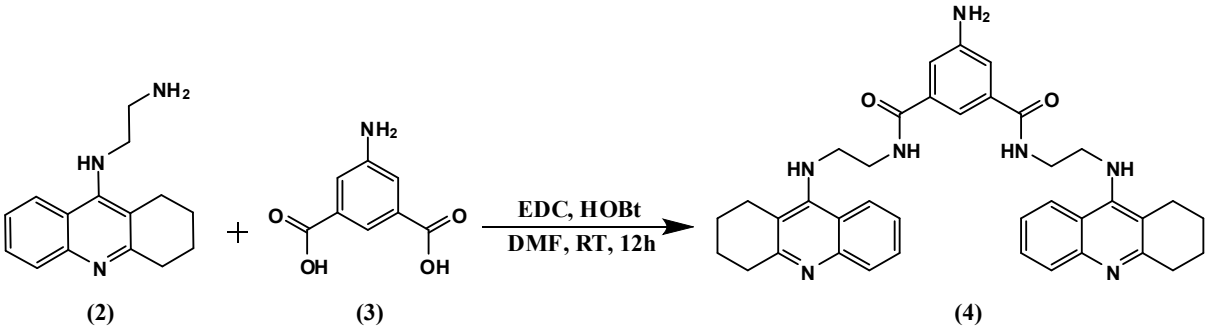

Scheme 2. Synthesis scheme of 5-amino-N^1,N^3-bis(2-(1,2,3,4-tetrahydroacridin-9-ylamino)ethyl)isophthalamide **(4)** by condensation of 5-Aminoisophthalic acid **(3)** and 9-aminoalkylamino-1,2,3,4-tetrahydroacridine **(2)**. Reagents and conditions: EDC, HOBt, anhydrous DMF, DIPEA, RT, 12h.

AChE and BuChE inhibition studies

AChE human (E.C.3.1.1.7, recombinant protein expressed in HEK293 cells), BuChE human (E.C.3.1.1.8, from human serum), 5,5'-Dithiobis(2-nitrobenzoic acid) (DTNB, Ellman's reagent), Acetylthiocholine (ATC), Butyrylthiocholine (BTC) were purchased from Sigma-Aldrich (Germany). OD and kinetic OD measurement were done in 24-well plate on Biotek H4 Hybridmulti-plate reader system, USA. The reference inhibitory drugs Tacrine (THA) was purchased from Sigma-Aldrich (Germany) and Bis(7)-tacrine from Tocris, Bristol, UK.

All the stocks of AChE (5U/mL), BuChE (5U/mL), DTNB (10mM), Acetylthiocholine (ATC, 3mM), and Butyrylthiocholine (BTC, 3mM) were prepared in 0.1M phosphate buffer (pH-7.0). The stocks of the test compounds were prepared in 10% ethanol (C_2H_5OH) in same 0.1M phosphate buffer (pH-7.0) in final volume of 1mL, and various concentrations of the test compounds ranging from 10^{-4}M – 10^{-15} M were prepared and tested in the following mentioned procedure by Ellman's method. [30]

In vitro enzyme inhibitor potency of the synthesized molecules THA,**(2),** Bis(7)-tacrine and **(4)**,and all intermediate derivatives were evaluated by Ellman's method. The enzymatic reaction mixture was prepared in a 24 well plate system, which constitutes AChE (0.0788U/mL), DTNB (315.45μM) and final volume of the reaction mixture was 634 μL. The enzymatic reaction was initiated by addition of ATC in mixture at final concentration of 473.18 μM at 37±0.5˚C in 0.1M

phosphate buffer (pH-8.0). The optical density (O.D) was measure at 412 nm in 15 s interval for total time period of 5 min in Synergy HT hybrid multi-plate reader. The initial enzymatic rate (Δ O.D/min) was determined by linear regression analysis of the absorbance vs time curve in more than triplicate (n ≥ 3). The initial enzymatic rate without inhibitor (R_0) corresponds to 100% enzymatic activity, and initial enzymatic rate in presence of various concentrations of inhibitor (R_i) were determined. The percentage enzyme activity in absence or presence of inhibitor was calculated by expression of % enzyme activity = (R_i/R_0) x 100. In case of determining initial enzymatic rate with known standard inhibitor, the above reaction mixture was mixed with standard inhibitor at various concentrations and allowed to stand the mixture at room temperature (RT) for 4.5 min. Similarly, enzymatic reaction was initiated by adding ATC to the mixture at concentrations mentioned above. All readings of initial rate in presence of standard inhibitor were taken in more than triplicate (n ≥ 3). For determining the background non-enzymatic rate, the mixture follows the same above-mentioned procedure while replacing the enzyme solution by buffer solution. The enzyme activity was plotted against the log concentration values of the inhibitor. Non-linear regression analyses were done on the curve to determine the IC_{50} values of the various synthesized ligands by using GraphPadPrism software (version 5.0).

BuChE inhibition studies were also performed by same procedure reported above, while using BuChE and BTC at same concentration at place of enzyme and substrate respectively. Similarly, the enzyme activity was plotted against log concentration values of inhibitors, and non-linear regression analysis was done to determine the IC_{50} values of various synthesized ligands by using GraphPadPrism software (version 5.0).

AChE and BuChE kinetic analysis

The kinetic measurement of the enzyme was evaluated at different concentrations of substrate were: 15.6 μM, 31.25 μM, 62.5 μM, 125 μM, 250 μM, 500 μM. The absorbance was measured

at different substrate concentrations in presence of inhibitor at concentration range (0–80 nM) to determine the K_m and V_{max} by non-linear regression analysis of the substrate-velocity curves. The double reciprocal plots or Lineweaver-Burk plots were made between inverse of substrate concentration [1/S] and inverse of initial reaction rate [$1/V_0$] for better illustration purposes, accurate values of K_m and V_{max} can also be calculated by double reciprocal plots. All the data processing was done using GraphPadPrism 5 software (version 5.0).

Thioflavin T competition assay

Thioflavin T and hAChE (Recombinant expressed in HEK293 cells) were purchased from Sigma-Aldrich (Germany). Fluorescence readings were recorded at room temperature (22.0 ± 2.0˚C) using Synergy H4 Hybrid multi-plate reader (Biotek, US). The fluorescence readings of mixture solutions were made at 448nm and 488nm for excitation and emission respectively. The PAS inhibitory activity of compound **(4)** was evaluated by a procedure described previously. [31]A solution of recombinant hAChE (500μM) in 50 mM glycine-NaOH buffer (pH-8.5) was incubated at room temperature for 24 h on stirring. After incubation, an aliquot of enzyme was added to a solution of Thioflavin T to a final concentration of 180 μM and 15 μM respectively in 50 mM glycine-NaOH buffer (pH-8.5). The solution was further incubated at room temperature with stirring for another 1 h and fluorescence was recorded *(F_1)*. To evaluate the potency of inhibitors to inhibit PAS, a solution of hAChE, Thioflavin T and inhibitor was incubated to a final concentration of 180 μM, 15 μM and 15 μM respectively in 50 mM glycine-NaOH buffer (pH-8.5) at room temperature for 1 h. And the corresponding fluorescence was measured *(F_2)*. Finally, fluorescence of control solution containing Thioflavin T to a final concentration of 15μM was recorded after incubation for 1 h in 50mM glycine-NaOH buffer (pH-8.5) on stirring *(F_0)*. The percentage reduction of Thioflavin T fluorescence was calculated as

AChE induced Aβ aggregation inhibition

Human amyloid β protein fragment 1-42 trifluoroacetate salt (0.1mg), 1,1,1,3,3,3-hexafluoro-2-propanol (HFIP) and absolute DMSO were purchased from Sigma-Aldrich (Germany).Human amyloid β protein fragment 1-42 trifluoroacetate salt was (0.1 mg, Sigma-Aldrich, USA) dissolved in HFIP at a concentration of 1 mg/mL.The amyloid aggregation inhibition properties of compound **(4)** and standard inhibitors were tested as per procedure described previously.[31] The peptide suspension was vortexed at 4ºC for 2 h, followed by sonicated for 15 mins creating a clear suspension of peptide in HFIP solution. The mixture was sealed and left overnight at 4ºC, next day the HFIP was removed by bubbling of nitrogen gas in the vial leaving a thin clear film on the wall of the vial. The sample was dissolved in DMSO, and aliquots of 4μL each were stored at -20ºC until needed for experiment. The peptide aliquot 4μL was further reconstituted in 100mM phosphate buffer (pH-8.0) at a final concentration of 230μM. For co-incubation experiments, 16μL of the hAChE with Aβ (final concentration of 2.30μM, Aβ/AChE molar ratio of 100:1) and hAChE with Aβ in presence of 2μL of synthesized inhibitor (final concentration of 100μM) in 100mM phosphate buffer (pH-8.0) were added. The final volume of the reaction mixture was 20μL, for measurement of amyloid fibril formation Thioflavin T (ThT) was added at a final concentration of 2.5μM in total volume (120μL) of the solution. Blanks containing $A\beta_{1-42}$, hAChE alone and $A\beta_{1-42}$ with tested inhibitor (final concentration 100μM) were taken separately. The fluorescence intensities were taken at λ_{ex} = 446nm &λ_{em}= 490nm which are characteristic of ThT bound to β-sheet of amyloid fibrils. The percent inhibition of the AChE-induced aggregation inhibition by tested compounds were calculated according to the following expression: 100 – $[(IF_i/IF_0) \times 100]$, where IF_i and IF_0 are fluorescence intensities obtained for $A\beta_{1-42}$ with AChE in presence and absence of the tested inhibitor respectively.

AFM imaging of AChE induced amyloid aggregation inhibition

The peptide aliquot 4μL was reconstituted in 100mM phosphate buffer (pH-8.0) at a final concentration of 230μM. For AFM analysis of AChE induced amyloid aggregation, 16μL of the

hAChE with Aβ (final concentration of 2.30μM, Aβ/AChE molar ratio of 100:1) and hAChE with Aβ in presence of 2μL of synthesized inhibitor (final concentration of 100μM) in 100mM phosphate buffer (pH-8.0) were added. The final volume of reaction mixture was 20μL. The samples for AFM imaging were prepared by loading a droplet of mixture solution (10-15μL) directly on fresh mica and left for incubation for 15-20 mins in a small container chamber, gently rinsed with buffer (10mM Tris, 5mM EDTA, 10mM KCl, 0.05% NaN_3, pH-7.4) and transferred to AFM microscope for image acquisition was done BioScope Catalyst Atomic Force Microscope (AFM) machine by Bruker.

Cytotoxicity studies

DMEM-F12 powdered media, Neuronal Media, N2 supplement, Propidium iodide (PI), cytosine arabinofuranoside (AraC), 4'6-diamidino-2-phenylindole (DAPI), Triton X-100, Trypsin and Diastase were purchased from Sigma-Aldrich (Germany). Horse serum and fetal bovine serum were purchased from Gibco, USA. Poly-L-lysine coated 6-well plates and 40μ cell strainer were purchased from BD.In vitro viability assay was performed on hippocampal neurons isolated from adult mice brain and which were grown in poly-L-lysine coated 6-well plates with neuronal culture media with 10% horse serum, 5% fetal bovine serum and N2 supplement. Initially, mice were anaesthetized and sacrificed by as per IAEC norms and approved protocols. Later on, brain were excised and both hippocampi from 4 adult mice were isolated under a stereomicroscope. Isolated hippocampus were immediately transferred to 4ºC in artificial CSF solution. Later to collection, all the hippocampi were subjected to diastase treatment and kept at 37˚C for 15 min to release individual cells from the hippocampus tissue. This resulting solution was further pipetted to make single cell suspension and passed through a 40μ cell strainer. Cell strainer passed solution was centrifuged and cells were washed twice with neuronal media and resuspended in complete neuronal media containing N2 supplement. These resuspended cells were then plated onto the poly-L-lysine coated 6-well plates at a density of 10000 cells/well in

3mL of media. For next 21 days, daily attached cells were washed twice with Mg^{+2} and Ca^{+2} free artificial CSF and consumed media was discarded and new media was replenished (2mL fresh + 1mL consumed). Once the cultures become mature, they were treated with 1μMcytosine arabinofuranoside (AraC) overnight to remove all the non-neuronal cells. The viability of the cells were determined on the basis on PI (propidium iodide) exclusion assay. The neuronal cells were treated with different concentrations of tested inhibitor in triplicate for 24h. After 24h, cells were incubated with PI (10μg/mL) and 300nM 4'6-diamidino-2-phenylindole (DAPI) as a counter stain to stain nuclei of the cells. The cells were incubated with both the dyes for 30min, and were fixed with 4% paraformaldehyde solution and permeabilized by 0.1% Triton X-100 solution. Fluorescence reading were taking in Synergy HT hybrid multi-plate reader with excitation at 544nm and emission 612nm for PI. The healthy cells which has intact plasma membrane were able to exclude PI, while their nuclei were stained blue by DAPI. The non-viable cells were positive for PI while retaining the DAPI in their nuclei, this indicate more PI uptake by the dead cells as compared to live cells. The viability was also monitored morphologically, where dead cells become rounded in shape as compared to viable cells which retain their neuronal phenotype.

Cell cycle analysis

Cell cycle analysis was performed on the neural tissue cells isolated from adult mice brain suspended in neuronal culture media with 10% horse serum, 5% fetal bovine serum and N2 supplement by using flow cytometry technique. Briefly, hippocampi from four adult mice brain were isolated, the tissue was subjected to diastase and trypsin treatment which was further converted to single cell suspension by gentle pipetting.The single cell suspension were passed through a cell strainer (40μ pore size). The collected suspension was centrifuged, washed twice with PBS and cells were resuspended in fresh media at a density of 5×10^5 cells/vial containing desired concentration of the inhibitor tested. All the cells treated with different concentrations of

inhibitor were incubated for 3h at 37˚C with humidified 5% CO_2 environment in incubator. Post 3h, the cells were again centrifuged, washed twice with PBS and were resuspended in fresh complete media without inhibitor. Cells were then acquired for cell cycle analysis in flow cytometer and analyzed by BD Accuri C6 system with software.

Molecular Docking studies

All the computational studies were performed using Schrödinger Software; Maestro 9.7 (Schrödinger, LLC, New York, NY, 2014); maestro 9.5 Prime version 2.3, Ligprep Version 2.9, Glide version 6. The crystal structure of *Torpedo Californica* Acetylcholinesterase Complexed With Alkylene-Linked Bis-Tacrine Dimer (7 Carbon Linker) Resolution of 2.15 Å, Species Torpedo Californica; PDB: 2CKM was subjected to Protein Preparation Wizard which includes pre-processing by assigning bond orders, addition of hydrogen and deletion of water molecules beyond 5 Å from hetero (het) groups and further minimization and optimization of protein structure was performed in the presence of force field OPLS2005.[32] Docking were performed on the crystal structure data of *torpedo californica* acetylcholinesterase, the docking was compared between the compound **(4)** and Bis(7)-tacrine for dual site binding in the enzyme pocket sites[33]. The grid was prepared according to the Bis(7)-tacrine binding site coordinates in the torpedo acetylcholinesterase and subjected to docking with analysis done with help of Schrodinger software. The grid formation was chosen in the area encompassing CAS (Trp 84, Phe 330, His 440) and PAS (Trp 279, Tyr 70, Ile 275). And for all the docking procedure, default settings were used for the all evaluated molecules.

Results and Discussion

Synthesis. Synthesis of compound **(4)** was carried out in three-step procedure. In the first step, Anthranilic acid was condensed with cyclohexanone at high temperature to yield 9-chloro-1,2,3,4-tetrahydroacridine **(1)** with 94% yield**.** Second step involves preparation of 9-

aminoalkylamino-1,2,3,4-tetrahydroacridine **(2)** was prepared by amino alkylation of 9-Chloro-1,2,3,4-tetrahydroacridine **(1)** in presence of phenol and sodium iodide as previously reported in the literature.[34] In the last step, final product **(4)** was efficiently synthesized by the condensation of 9-aminoalkylamino-1,2,3,4-tetrahydroacridine with **(3)** (5-Aminoisophthalic acid, 5-AIA) via EDC/HOBt coupling procedure with 30.2% yield as previously reported procedure.[35] The compound **(4)** can further provide site for functionalization with reporter groups as well for various applications.

AChE and BuChE inhibition

The inhibitory potential of various tacrine derivatives were evaluated by ellman's colorimetric assay. The catabolic reaction of acetylthiocholine (ATC) was intiated by AChE in the presence of a chromogenic substrate,5'5-dithiobis (2-nitrobenzoic acid) (DTNB).

(a) (b)

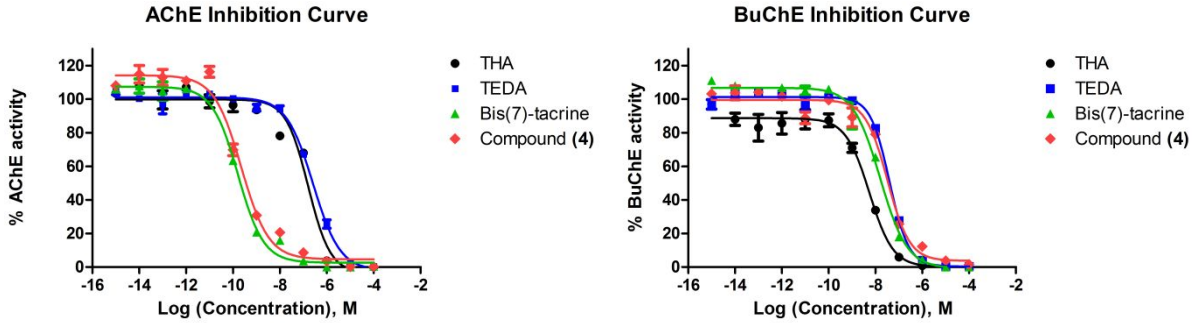

Fig.3 Enzyme inhibition curve of THA, TEDA, Bis(7)-tacrine and compound **(4)** on AChE (a) and BuChE (b) in concentration range (100μM – 1fM) of inhibitor tested.

For measuring potency of inhibitor, enzymatic activity was evaluated at various concentrations in the presence or absence of the inhibitor. The initial reaction rate were determined by using ΔOD_{412}/min from optical density versus time curves for various concentrations in prescence or absence of inhibitor respectively. All the IC_{50} values were calculated from non-linear regression analysis of the % AChE/BuChE activity versus concentration of inhibitor using graphpad prism

5.0. All the tacrine derivatives synthesized were shown to be very potent inhibitors of the AChE and BuChE in subnanomolar concentrations in vitroexperiments with IC_{50} values ranging from 100 nM to 0.2 nM were represented in **Fig.3**. The dimeric molecule **(4)** exhibited more potency for AChE and BuChE as compared to THA, **(2)** but similar to Bis(7)-tacrine. The IC_{50} values for different derivatives synthesized along with THA and Bis(7)-tacrine were depicted in **Table 1**. The AChE IC_{50} value of THA, TEDA, Bis(7)-tacrineand compound **(4)** were determined

Table 1. Results of inhibition assay of reference and synthesized derivatives of tacrine and their selectivities are expressed as the ratios of IC_{50} values.

Compound	Structure	AChE IC_{50} (nM)	BuChE IC_{50} (nM)	Selectivity BuChE IC_{50}/AChE IC_{50}	Hill Slope AChE	Hill Slope BuChE
THA	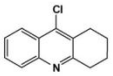	184.6 ± 1.2	6.57 ± 1.2	0.035	0.70	0.59
TEDA	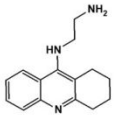	229.1 ± 1.2	59.84 ± 1.1	0.261	0.78	0.91
Bis(7)-tacrine	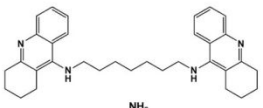	0.33 ± 0.04	15.78 ± 1.2	47.81	1.24	0.61
Compound **(4)**	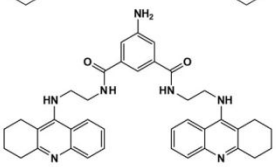	0.54 ± 0.06	32.49 ± 1.2	60.16	1.42	0.67

as 184.6 ± 1.2, 229.1 ± 1.2, 0.33 ± 0.04 and 0.54 ± 0.06 nM, while on BuChE were6.57 ± 1.2, 59.84 ± 1.1, 15.78 ± 1.2 and 32.49 ± 1.2 nM respectively. The selective inhibition of AChE was also calculated for reference and tacrine derivative compounds by ratios of IC_{50} of BuChE/AChE. THA, TEDA, Bis(7)-tacrine and compound **(4)** showed selective ratio of 0.035, 0.261, 47.81 and 60.16 respectively, this suggest the highest selectivity of compound **(4)** towards AChE. Being the homodimeric inhibitor, we also evaluated the hill slope of the AChE and BuChE inhibition mechanism. THA, TEDA, Bis(7)-tacrine and **(4)** shows hill cofficient of

0.70, 0.78, 1.24 and 1.42, this suggests the higher binding and cooperative binding of the dimeric inhibitors as compared to monovalent inhibitors.

AChE and BuChE kinetic analysis

To study the inhibitory mechanism of prepared tacrine derivative **(4),** kinetic inhibition studies were performed with varying substrate and inhibitor concentrations, and substrate-velocity curve or Lineweaver-Burk plots were generated.The Lineweaver-Burk curve for bivalent inhibitor **(4)** was represented by **Fig.4** (a) and (b), this curve gives V_{max} value (i.e. reciprocal of the Y intercept) and K_m value (i.e. negative reciprocal of X intercept), but V_{max} cannot be calculated

(a) (b)

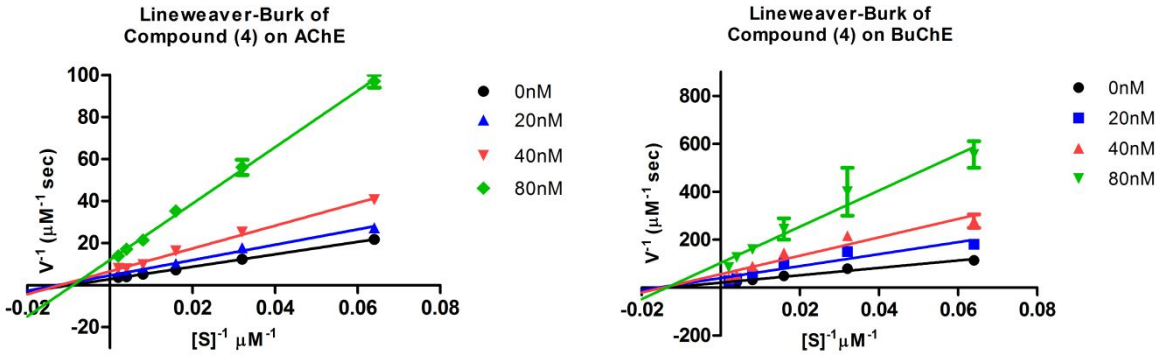

Fig. 4 The Lineweaver-Burk plot of compound **(4)** on AChE (a) and BuChE (b) in a concentration range of compound **(4)** was ranged (0-80 nM) and substrate concentration (ATC) was ranged (15.625-500 µM).

due to non-extrapolation of graph to infinity in Michaelis-Menton curves. So for better clarity and illustration reciprocals of velocity and substrate were plotted in the form of Lineweaver-Burk plots shown in **Fig. 4**. The Lineweaver-Burk plot gives V_{max} and K_{max} values for compound **(4)** which were found to be 0.3594 µM sec^{-1} and 106.47 µM for AChE, while V_{max} and K_m for BuChE were 0.0481 µM sec^{-1} and 74.23 µM respectively. It was also seen from observed data that, with increase in concentration of compound **(4)** the V_{max} value decreases and K_m value remains approximately the same, this suggests the mechanism of inhibition of AChE and BuChE was non-competitive type.

Thioflavin T competition assay

The previous data about compound **(4)** were suggestive of cooperative binding with both the available site in the gorge of AChE, i.e. CAS and PAS. It was also assumed that only AChE have PAS, while BuChE lacks this additional binding site. Therefore, compound **(4)** also explored forits ability to inhibit the PAS, which is the site reported to accelerate the amyloid

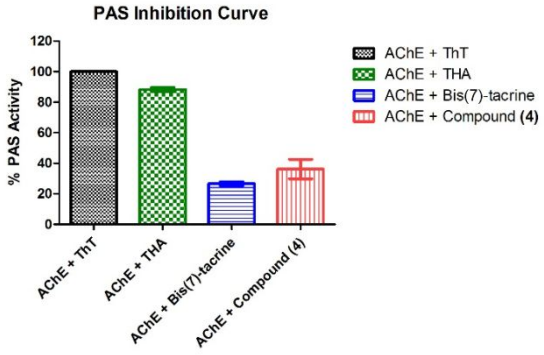

Compound	% PAS activity (Mean ± SEM)
ThT	100 ± 0
THA	88.28 ± 1.4
Bis(7)-tacrine	26.65 ± 1.3
Compound **(4)**	36.19 ± 6.3

Fig. 5 Peripheral active site (PAS) inhibition potential of various tacrine derivatives was evaluated by releasing ThT from PAS of AChE. Results were expressed as percentage inhibition of PAS activity, the values represents mean value with standard error mean of more than triplicate (n ≥ 3).

Peptideaggregation supposed to be one of the major event in AD pathology. PAS inhibition assay for THA, Bis(7)-tacrine and compound **(4)** was performed on human AChE. ThT reported to bind to PAS site of the AChE which leads to increase in fluorescence of ThT in the bound form. A reduction in ThT fluorescence was measured as the parameter for replacing ThT from the PAS of AChE, which would give the measure of inhibition of PAS activity. THA, Bis(7)-tacrine and compound **(4)** showed 88 ± 1.4, 26.65 ± 1.3 and 36.19 ± 6.3 percent of PAS activity respectively shown in **Fig 5.** The maximumreduction in PAS activity was achieved by Bis(7)-tacrine, while that of compound **(4)** was slightly lesser then Bis(7)-tacrine. These data suggests that compound **(4)** has shown equally potent dual binding site inhibitorwhich can inhibit PAS site of the enzyme effectively. Compound **(4)** presumably inhibit the CAS as well as PAS both the

sites simultaneously, which was expected from molecular modelling data of compound **(4)** with AChE.

AChE induced Aβ aggregation inhibition

As previously stated in many reports that, PAS of AChE facilitates and accelerate the aggregation of the amyloid peptide in AD brain. This event could be considered as the core mechanism by which amyloid peptide leads to multifactorial disease condition. Therefore, we evaluated its potency in inhibiting the AChE induced amyloid peptide aggregation in vitro. In this assay, ThT was used as native dye which binds to aggregated form of amyloid peptide and shows enhanced fluorescence as compared to unbound ThT. A decrease in ThT fluorescence was considered as parameter for inhibiting AChE induced amyloid aggregation of the tested compound. A single concentration of 100μM was selected for better comparison in inhibiting potential of all the reference drugs and prepared compounds. THA, Bis(7)-tacrine and compound**(4)**were tested for, their ability to inhibit amyloid aggregation.

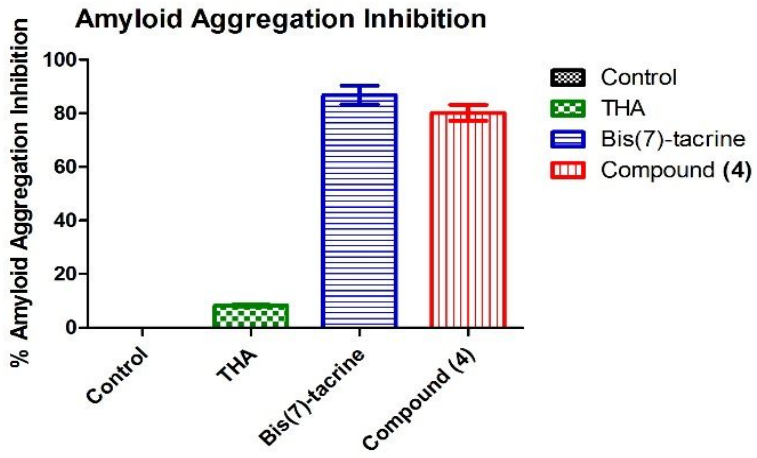

Compound	% Amyloid Aggregation Inhibition at 100μM (Mean ± SEM)
Control	0
THA	8.3 ± 0.32
Bis(7)-tacrine	86.8 ± 3.45
Compound **(4)**	80.16 ± 2.94

Fig.6 Amyloid aggregation inhibition potential of tacrine derivatives were evaluated. Potency were measured as parameter of reducing fluorescence of bound ThT. All derivatives were evaluated at a concentration of 100μM. Aggregation inhibition expressed as percentage compared to control values, the values represents mean value with standard error mean of more than triplicate(n ≥ 3).

Results have shown that amyloid aggregation was inhibited by THA, Bis(7)-tacrine and compound **(4)** at 100μM was 8.3 ± 0.32, 86.8 ± 3.45 and 80.16 ± 2.94 percentage as compared to the control respectively shown in **Fig. 6**. However, these results indicate compound **(4)** as equally potent inhibitor as compared to Bis(7)-tacrine in inhibiting AChE induced amyloid aggregation.

AFM imaging of AChE induced amyloid aggregation inhibition:

As indicated from previous data, that selected inhibitors Bis(7)-tacrine and compound **(4)** were shown to the most potent inhibitors for AChE induced amyloid aggregation. Therefore, AFM image acquisition were done on mixtures containing Bis(7)-tacrine and compound **(4)** while comparing to the control aggregation process **Fig 7**. The AFM images reveals and correlated with the data obtained using decrease in ThT fluorescence in the previous experiments. The compound **(4)** shows aggregation inhibition to extent similar like Bis(7)-tacrine.

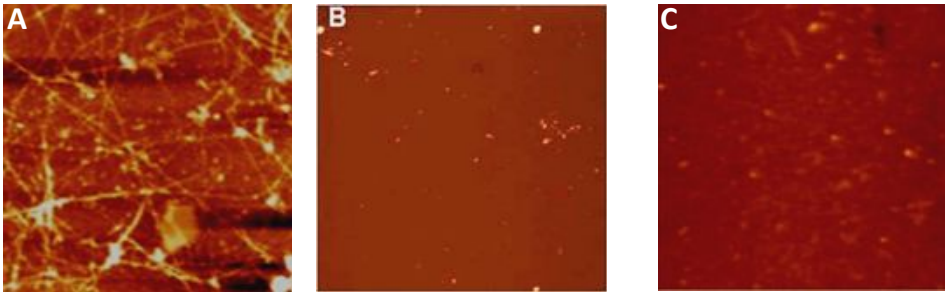

Fig 7 A) Atomic Force Microscopy (AFM) of amyloid aggregation $A\beta_{1-42}$ fibrils **B)** Inhibtion of aggregation by Bis(7)-tacrine **C)** Inhibtion of aggregation by Compound (**4**)

Cytotoxicity studies

From *in vitro* data of previous studies suggest compound **(4)** as equally potential inhibitor of AChE/BuChE activity, PAS activity and AChE induced amyloid aggregation, but it is very much needed to evaluate the overall toxicity of this compound on cells of neuronal tissue. Therefore,

cytotoxicity of the Bis(7)-tacrine and compound **(4)** was evaluated by PI exclusion assay on hippocampal neurons at various concentration of treatment (**Fig 8**). Both Bis(7)-tacrine and compound **(4)** were non-toxic up to concentration of 200μM, but as the concentration increases further Bis(7)-tacrine started to show cytotoxicity at 300μM while compound **(4)** started to show cytotoxicity at 400μM. The percentage cellular viability at 300μM of bis(7)-tacrine treatment

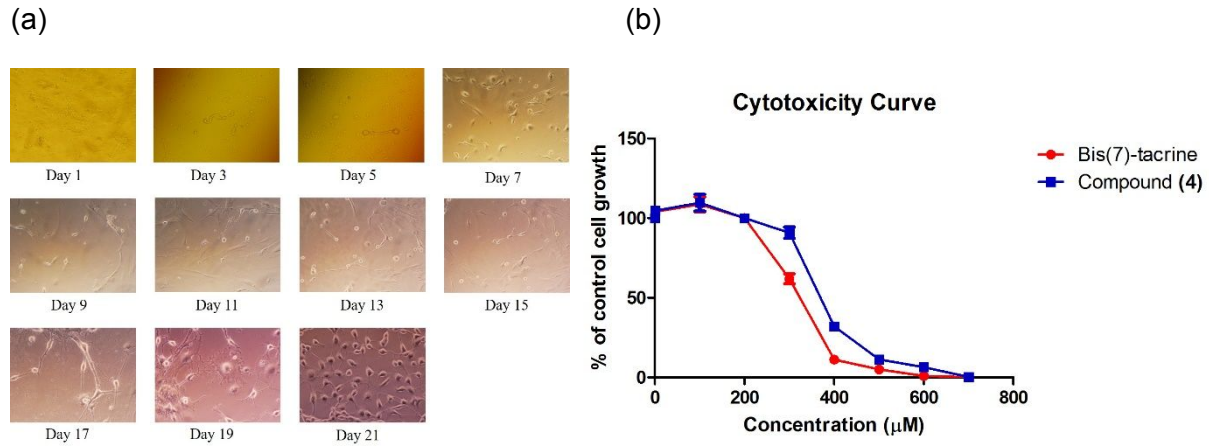

Fig. 8 (a) Isolation and culturing of primary hippocampal neuronal cultures from adult mice brain. (b) Cellular cytotoxicity of compound **(4)** on primary hippocampal neuronal cultures was evaluated with the reference inhibitor Bis(7)-tacrine. Percentage of control cell growth was plotted against concentration range (0 – 700 μM). The the values represents mean value with standard error mean of more than triplicate(n ≥ 3).

was 65%, while of compound **(4)** was 90%. The IC_{50} values for Bis(7)-tacrine and compound **(4)** on hippocampal neurons were ≈320μM and ≈385μM. These findings suggests the non-toxic nature of the compound **(4)** to further explore this ligand as therapeutic ligand without causing significant cytotoxicity on neuronal tissue, therefore both the ligands could be used as potential inhibitors for treatment of AD pathology in clinics.

Cell cycle analysis

In continuation to cytotoxicity evaluation, we also tried to check the effect of compound **(4)** on cell cycle. Most of anti-Alzheimer's drugs having neurogenic potential as they not only mitigate the AD insult but also induce cellular multiplication. Therefore, we also explored the neurogenic potential of compound **(4)** as compared to Bis(7)-tacrine. In the present assay, fraction of cells present in different phases of cell cycle were measured, more fraction of cells in S-phase represents more amount of cellular synthetic activities leads to cellular multiplication. **Fig. 8** represents the results of cell cycle analysis, which reveals cell cycle variations at different concentration of the inhibitor tested. Upper panel represents cells treated with different concentrations of Bis(7)-tacrine, while the lower shows the cells treated with compound **(4)**. Theupper control panel shows percent of total cells in G_1, S and G_2/M phases were 53.5%, 16.7% and 20.7% respectively, while the lower control panel shows 56.8%, 13.1% and 19.9% respectively. Comparison of both control panel suggest that approximately equal fraction of cells in all three phases.But when Bis(7)-tacrine and compound **(4)** were introduced at 150μM concentration, the cells in G_1 phase increases to 62.7% in Bis(7)-tacrine, while in case of compound **(4)** it remains similar to control at 51.0%. The S-phase in Bis(7)-tacrine reduces to 10.9%, whereas in compound **(4)** it increases to 15.4%, and cells in G_2/M phase decreased to8.6% in Bis(7)-tacrine whereas it remains same in compound **(4)** at 19.9%. When both Bis(7)-tacrine and compound **(4)** introduced at 300μM, the G_1, S and G_2/M phases were 67.1%, 6.6%, 8.2% and 63.4%, 14.4%, 9.1% respectively,it is worthwhile to note that there was more than 2-fold increase in S-phase population at higherconcentration of compound **(4)** as compared to Bis(7)-tacrine. At concentration of 800μM, G1, S and G2/M phases were 80.0%, 6.6%, 3.1% and 77.7%, 14.0%, 2.8% in case of Bis(7)-tacrine and compound **(4)** respectively.

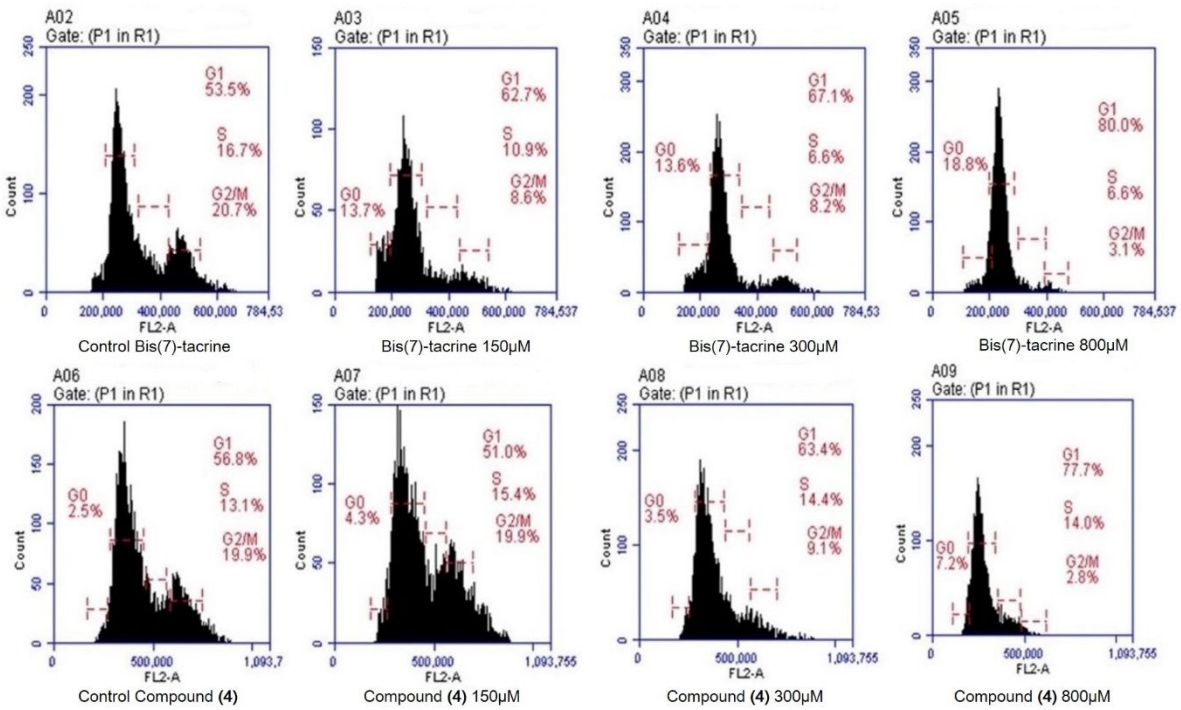

Fig. 9 Comparison profile of cell cycle analysis by flow cytometry. Upper Panel shows cells in different cell cycle phases after Bis(7)-tacrine treatment, While lower panel shows fraction of cells after treatment with compound **(4)** at different concentrations.

These observations suggest induction of more population of cells in S-phase when subjected to pharmacologically active concentration of the compound **(4)** as compared to Bis(7)-tacrine

Molecular Docking studies

Three-dimensional molecular modelling was performed to assess the binding affinity of the newly synthesized compound **(4)** and compared with Bis(7)-tacrine and other reported potent inhibitors on the active site of the AChE.[32,34] Both static and dynamic molecular docking was performed using 2CKM (*Torpedo Californica* Acetylcholinesterase complexed with alkylene-linked Bis-Tacrine Dimer (7 Carbon Linker) Resolution of 2.15 Å, Species *Torpedo Californica)*. Bivalent ligand approach have been known for AChE inhibitors because of the favorable

(A)

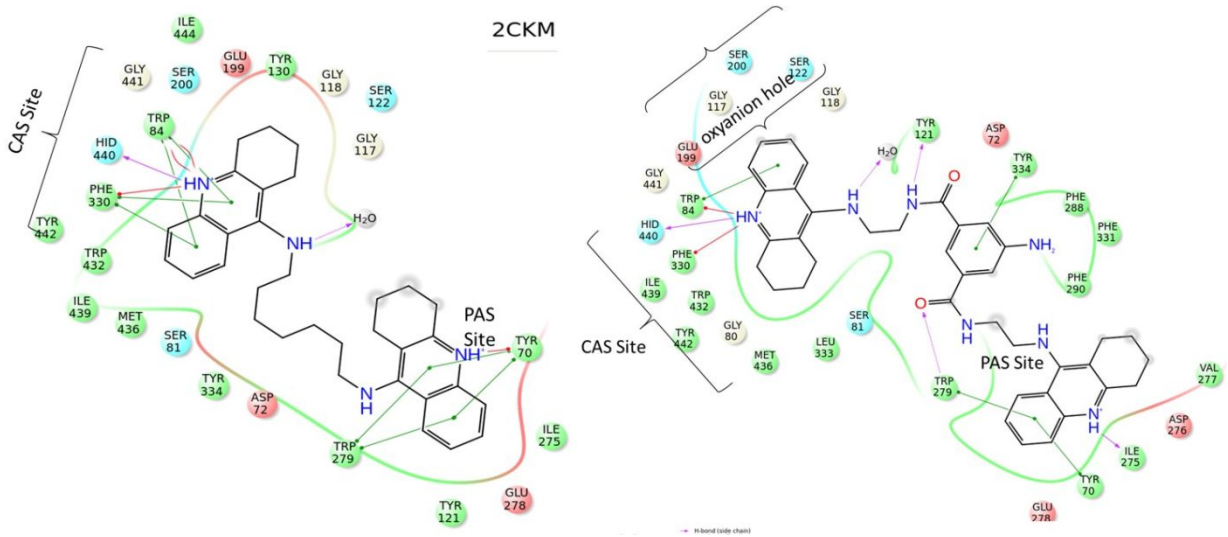

Fig. 10 The two dimensional interaction pattern of Bis(7)-tacrine and compound **(4)**on the amino acid residues of AChE of *Torpedo californica* where green colored are hydrophobic, cyan are polar, red are negative and purple are positive amino acid residues. Pink lines shows the hydrogen bonds while green lines represents π – cation interactions.

Geometric consideration of the active site gorge of AChE where two binding site were present at the extreme ends in the form of CAS and PAS. In the present docking study, the docking pattern of Bis(7)-tacrine was compared with compound **(4)**, which showed more number of interactions due to aromatic linker in compound **(4)** as compared to alkyl linker in Bis(7)-tacrine. The tricyclic pharmacophores in both ligands resides in the expected location of CAS and PAS. The green lines show the hydrophobic interactions including π-π and stacking interactions, while the pink line shows the hydrogen bond interactions. The pharmacophores in both theligands interacts with the key residues of CAS were Trp84, Phe330 and His440, the aromatic cationic nitrogen also forms hydrogen bonds with Phe330 and His440. Similarly, if we analyzethe interaction of anotherpharmacophore which resides in the PAS of AChE in both the ligands,this shows that Bis(7)-tacrinehaving hydrophobic interactions with Tyr70 and Trp279 and aromatic cationic nitrogen having hydrogen bond with Tyr70. But if we see the interaction profile of PAS residing pharmacophore in compound **(4)** reveals additional interaction with Ile275. In the compound **(4)**the aromatic linker was introduced to provide an additional site for radiolabeling, but the

aromatic and two amide bonds provides additional set of interactions which would lead to enhanced docking and glide score**Fig. 10.**Two amide bonds were involved in formation of hydrogen bonds with Tyr121 and Trp279, while the aromatic ring made π-π and stacking interactions with Tyr334. We have also compared the docking and glide scores of other reported ligands with compound **(4)** given in the **Table 2**.

Table 2. Molecular docking analysis of various reference tacrine derivatives with compound **(4).** The results are expressed here as percentange of scores of tacrine derivatives mentioned here with respect to Bis(7)-tacrine.

Compound	Structure	Docking Score (Percentage with respect to Bis(7)-tacrine)	Glide Score (Percentage with respect to Bis(7)-tacrine)
Bis(7)-tacrine		0.00	0.00
11b	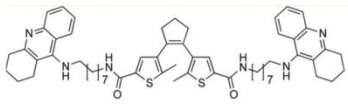	-12.11	-12.10
Compound **(4)**	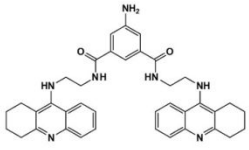	4.27	4.27

Therefore, the study conclude that compound **(4)** has highest binding affinity towards AChE in molecular docking studies which in turn lead us to synthesize compound **(4)** and evaluate its potential as AChE inhibitor.

Discussion

In the present study, we described the design, synthesis and its biological evaluation of compound **(4)** as a potential inhibitor of AChE, which further could be utilized as a tracer molecule to detect fluctuation of AChE expression levels in different regions of the brain in disorders involving AChE. In the current work, we merged two different approaches for making a successful tracer molecule which should retain its therapeutic potential as well while used for

molecular imaging applications. [33] According to cholinergic hypothesis, enhancement of acetylcholine at junctional synapses significantly improves the cognitive functions, this fact further lead to synthesis of various classes of AChE inhibitors for treatment of AD. THA was the first drug approved by FDA for treatment of AD, so many more THA based derivatives were synthesized and evaluated. But due to low specificity THA was having multiple side effects. Therefore, Pang et al, (1996) designed and synthesized a novel catalytic active site structure based inhibitor Bis(7)-tacrine with subnanomolar potency[25]. Many reports also suggests that, Bis(7)-tacrine was the most potent inhibitor with high specificity towards AChE known to us till date. Therefore, we considered to make a homodimeric inhibitorhaving equal potency based imaging agent for tracing AChE in neurological disorders.

Many attempts were made to visualize AChE with the help of radiotracers in PET/SPECT imaging modalities. As far as radiotracers of AChE are concerned, they can be classified into two categories 1) AChE substrate based tracer and 2) AChE inhibitor based tracers. AChE substrate based tracers were not successful due to diffusion of radio labeled products inside the brain area, which in turn not suggestive of accurate location of AChE in different brain regions.[18] While the AChE inhibitor based radiotracers were much more stable and accurate in locating AChE in brain imaging.[22,23] So, here we tried to use homodimeric inhibitor of AChE coupled with radiotracer ability to design a theranostic ligand for treatment of AD which could lead to better patient management and monitoring the progression of the disease.

In the current synthesis, we have inserted an aromatic linker (5-aminoisophthalic acid) in a dimeric tacrine based inhibitor of AChE, which could provide an additional site to radiolabeling for imaging applications retaining the same subnanomolar potency of inhibiting AChE. The coupling procedure reported here is most convenient due to water solubility of side products which can be easily separated from the products by extraction procedure.[35] 5-AIA is often used as linker for making dimeric molecules, which contains two similar moieties connected to isophthalate linker. 5-AIA was previously employed in attaching two chelating moieties to the

biotin derivative for various applications including radio imaging. The presence of 5-amino group in the isophthalate linker provide an extra site for further functionalization with an optical or radioactive reporter (i.e. FITC or ^{11}C chemistry).

The enzyme inhibition and enzyme kinetics data suggests inhibitor properties for compound **(4)** which was having IC_{50} value in subnanomolar concentration with non-competitive kind of enzyme inhibition, which is very much similar to Bis(7)-tacrine mode of inhibition. Compound **(4)** also showed more positive cooperative binding of tacrine pharmacophore to active sites of AChE more than Bis(7)-tacrine. The PAS inhibition and amyloid aggregation data also reveals its potency for inhibiting the PAS site of AChE was equivalent to Bis(7)-tacrine. Evaluation of cytotoxic potential was also checked with comparison to Bis(7)-tacrine, compound **(4)** comes out to have less cytotoxicity effect on the hippocampal neurons. Apart from cytotoxicity, compound **(4)** was also found out to be of neurogenic potential through flow cytometry analysis. Compound **(4)** treated cells exhibited more fraction of cell population in the S-phase of cell cycle as compared to Bis(7)-tacrine, these data proves the neurogenic potential of compound **(4)**. Molecular docking analysis showed higher affinity of compound **(4)** for CAS and PAS as compared to Bis(7)-tacrine and other reported ligands. The preliminary evaluation of the compound **(4)** with its theranostic potential makes this ligand a promising PET imaging tracer for imaging AChE in vivo, which could open new avenues for diagnosis and therapy in Alzheimer's disease.

ASSOCIATED CONTENT

Supporting Information available: [**pp. 1S-8S**] NMR and Mass Spectra of compounds, Enzyme kinetic curves (Michaelis-Menton curve) of compound **(4)** on AChE and BuChE. This material is available free of charge via the internet at http://pubs.acs.org.

AUTHOR INFORMATION

Corresponding author

*E-mail: puja.hazari@gmail.com Tel: +91-01123905244 Fax: +91-01123919509

Notes

The authors declare no competing financial interest.

ACKNOWLEDGEMENTS

The present work was supported by Project INM 319, Defence Research and Development Organization, Ministry of Defence and CSIR, Delhi. The authors also extend their thank to the Director, INMAS and Prof. Ramesh Chandra, HOD, Chemistry Dept., Delhi University for providing necessary facilities.

References

1. Gauthier, S.; Reisberg, B.; Zaudig, M.; Petersen, R. C.; Ritchie, K.; Broich, K.; Belleville, S.; Brodaty, H.; Bennett, D.; Chertkow, H.; Cummings, J. L.; Leon, M. D.; Feldman, H.; Ganguli, M.; Hampel, H.; Scheltens, P.; Tierney, M. C.; Whitehouse, P.; Winblad, B. Mild cognitive impairment. *Lancet***2006**, 367, 1262–1270.
2. Mucke, L. Neuroscience: Alzheimer's disease. *Nature***2009**, 461,895 − 897.
3. Salmon, D. P.; Lange, K. L. Cognitive screening and neuropsychological assessment in early Alzheimer's disease. *Prog. Neurobiol.***2001**, 60, 139-165.
4. Glenner, G.G. The pathobiology of Alzheimer's disease. *Annu. Rev. Med.***1989**, 40:45–51.
5. Selkoe, D. J. Alzheimer's disease: genes, proteins, and therapy. *Physiol. Rev.***2001**, 81, 741–766.

6. Selkoe, D. J. The molecular pathology of Alzheimer's disease. *Neuron***1991**, 6,487–498.

7. Dickson, D. W. The pathogenesis of senile plaques. *J.Neuropathol. Exp. Neurol.***1997**, 56, 321–339.

8. Kayed, R.; Head, E.; Thompson, J.L.; McIntire, T.M.; Milton, S.C.; Cotman, C.W.; Glabe, C.B. Common structure of soluble amyloid oligomers implies common mechanism of pathogenesis. *Science***2003**, 300, 486-489.

9. Cleary, J.P.; Walsh, D.M.; Hofmeister, J.J.; Shankar, G.M.; Kuskowski, M.A.; Selkoe, D.J.; Ashe, K.H. Natural oligomers of the amyloid ß-protein specifically disrupt cognitive function. *Nat. Neuroscience***2005**, 8, 79-84.

10. Demuro, A.; Mina, E.; Kayed, R.; Milton, S.C.; Parker, I.; Glabe, C.G. Calcium dysregulation and membrane disruption as a ubiquitous neurotoxic mechanism of soluble amyloid oligomers. *J. Biol. Chem.***2005**, 280, 17294-17300.

11. Hampel, H.;Bürger, K.; Teipel, S. J.; Bokde, A. L. W.; Zetterberg, H.; Blennow, K. Core candidate neurochemical and imaging biomarkers of Alzheimer's disease. *Alzheimer's & Dementia***2008**, 4, 38-48.

12. Craig, L. A.; Hong, N. S.; McDonald, R. J. Revisiting the cholinergic hypothesis in the development of Alzheimer's disease. *Neuroscience and biobehavioural reviews***2011**, 35(6), 1397-1409.

13. Francis, P.T.; Palmer, A. M.; Snape, M.; Wilcock, G. K. The cholinergic hypothesis of Alzheimer's disease: a review ofprogress. *J. Neurol. Neurosurg. Psychiatry***1999**, 66 (2), 137–147.

14. Kasa P, Rakonczay Z, Gulya K: The cholinergic system in Alzheimer'sdisease. Prog. Neurobiol**1997**, 52:511–535.

15. Youdim, M. B.; Buccafusco, J. J. Multi-functional drugs for various CNS targets in the treatment of neurodegenerative disorders. *Trends Pharmacol. Sci.***2005**, 26, 27–35.

16. Zhang, H. Y. One-compound-multiple-targets strategy to combat Alzheimer's disease. *FEBS Lett.* **2005**, 579, 5260–5264.

17. Iyo, M.; Namba, H.; Fukushi, K.; Shinotoh, H.; Nagatsuka, S.; Suhara, T.;Sudo, Y.; Suzuki, K.; Irie, T. Measurement of acetylcholinesterase by positron emissiontomography in the brains of healthy controls and patients withAlzheimer's disease. *Lancet***1997**, 349, 1805-1809.

18. Kikuchi, T.; Okamura, T.; Zhang, M. R.;Irie, T. PET probes for imaging brain acetylcholinesterase. *J. Label Compd. and Radiopharm***2013**, 56, 172-179.

19. Kilbourn, M. R.; Snyder, S. E.; Sherman, P. S.; Kuhl, D. E. In Vivo Studies of Acetylcholinesterase Activity Using a Labeled Substrate, N-[^{11}C] Methylpiperdin-4-yl Propionate ([^{11}C]-PMP). *Synapse***1996**, 22, 123-131.

20. Ryu, E. K.; Choe, Y. S.; Park, E. Y.; Paik, J. Y.; Kim, Y. R.; Lee, K. H.; Choi, Y.; Kim, S. E.; Kim, B. T. Synthesis and evaluation of 2-[^{18}F] fluoroCP-118,954 for thein vivo mapping of acetylcholinesterase. *Nucl. Med. Biol.***2005**, 32, 185-191.

21. Prenant, C.; Couzel, C. Synthesis of [11C]-Sarin. J.Label. Compd. Radiopharm. **1990**,28, 645 − 651.

22. Planas, A. M.; Crouzel, C.;Hinnen, F.; Jobert, A.; Né, F.;DiGiamberardino, L.;Tavitian, B. Rat brain acetylcholinesterase visualized with [^{11}C]Physostigmine. *NeuroImage***1994**, 1(3), 173-180.

23. Vos, F. D.; Santens, P.; Vermeirsch, H.; Dewolf, I.; Dumont, F.; Slegers, G.; Dierckx, R. A.;Reuck, J. D. Pharmacological Evaluation of [^{11}C]Donepezil as Tracer forVisualization of Acetylcholinesterase by PET. *Nucl. Med. Biol.***2000**, 27, 745-747.

24. Bonnot-Lours, S.; Prenant, C.;Crouzel, C. Synthesis of9-[^{11}C]Methylamino-1,2,3,4-tetrahydroacridine, A Potent Acetylcholine Esterase Inhibitor. *Appl. Radiat. Isot.***1991**, 42, 690 – 691.

25. Pang, Y. P.; Quiram, P.; Jelacic, T.; Hong, F.; Brimijoin, S. Highly Potent, Selective, and Low CostBis-tetrahydroaminacrine Inhibitors of Acetylcholinesterase: STEPS TOWARDNOVEL DRUGS FOR TREATINGALZHEIMER'S DISEASE. *J. Biol. Chem.***1996**, 271, 23646-23649.

26. Cavalli, A.; Bolognesi, M. L.; Minarini, A.; Rosini, M.; Tumiatti, V.; Recanatini, M.; Melchiorre, C. Multi-target-Directed Ligands to Combat Neurodegenerative Diseases. *J. Med. Chem.***2008**, 51(3), 347- 372.

27. Więckowska, A.; Wichur, T.; Godyń, J.; Bucki, A,; Marcinkowska, M,; Siwek, A.; Więckowski, K,; Zaręba, P.; Knez, D,; Głuch-Lutwin, M,; Kazek, G.; Latacz, G.; Mika, K.; Kołaczkowski, M.; Korabecny, J.; Soukup, O.; Benkova, M.; Kieć-Kononowicz, K.; Gobec, S.; Malawska, B. Novel multi-target-directed ligands aiming at symptoms and causes of Alzheimer's disease. *ACS Chem. Neurosci.***2018**, 9 (5), 1195–1214.

28. Pi, R.; Mao, X,; Chao, X.; Cheng, Z.; Liu, M.; Duan, X.; Ye, M.; Chen, X.; Mei, Z.; Liu, P.; Li, W.; Han, Y. Tacrine-6-Ferulic Acid, a Novel Multifunctional Dimer, Inhibits Amyloid-β-Mediated Alzheimer's Disease-Associated PathogenesisInVitroAnd In Vivo.*PLoS ONE***2012**, 7(2): e31921.

29. Rizzo, S.; Bisi, A.; Bartolini,M.; Mancini, F.; Belluti, F.; Gobbi, S.; Andrisano, V.; Rampa, A. Multi-target strategy to address Alzheimer's disease: Design,

synthesisandbiological evaluation of new tacrine-based dimers. *Eur. J. Med. Chem.***2011**, 46, 4336-4343.

30. Ellman, G. L.; Courtney, K. D.; Andres, V.; JR. Featherstone, R. M. A new and rapid colorimetric determination of acetylcholinesterase activity. *Biochem. Pharmacol.***1961**, 7, 88-95.

31. Camps, P.; Formosa, X.; Galdeano, C.; Gomez, T.; Munoz-Torrero, D.; Scarpellini, M.; Viayna, E.; Badia, A.; Clos, M. V.; Camins, A.; Pallas, M.; Bartolini, M.; Mancini, F.; Andrisano, V.; Estelrich, J.; Lizondo, M.; Bidon-Chanal, A.; Luque, F. J. Novel Donepezil-Based Inhibitors of Acetyl- and Butyrylcholinesterase and Acetylcholinesterase-Induced β-Amyloid Aggregation. *J. Med. Chem.* **2008,** *51,* 3588–3598.

32. Rydberg, E. H.; Brumshtein, B.; Greenblatt, H. M.; Wong, D. M.; Shaya, D.; Williams, L. D.; Carlier, P. R.; Pang, Y. P.; Silman, I.; Sussman, J. L. Complexes of Alkylene-Linked Tacrine Dimers with Torpedo californicaAcetylcholinesterase:Binding of Bis(5)-tacrine Produces a Dramatic Rearrangement in the Active-Site Gorge. *J. Med. Chem.***2006**, 49, 5491 – 5500.

33. Gjerløff, T.; Jakobsen, S.; Nahimi, A.; Munk, O. L.; Bender, D.; Alstrup, A. K. O.; Vase, K. H.; Hansen, H. B.; Brooks, D. J.; Borghammer, P. In Vivo Imaging of Human Acetylcholinesterase Densityin Peripheral Organs Using 11C-Donepezil: Dosimetry,Biodistribution, and Kinetic Analyses. *J. Nucl. Med.***2014**, 55, 1818–1824.

34. Bolognesi, M. L.; Cavalli, A.; Valgimigli, L.; Bartolini, M.; Rosini, M.; Andrisano, V.; Recanatini, M.; Melchiorre, C.Multi-Target-Directed Drug Design Strategy:From a Dual Binding SiteAcetylcholinesterase Inhibitor to aTrifunctional Compound against Alzheimer's disease. *J. Med. Chem.***2007**, 50, 6446–6449.

35. Chen, X.; Wehle, S.; Kuzmanovic, N.; Merget, B.; Holzgrabe, U.; König, B.; Sotriffer, C. A.; Decker, M. Acetylcholinesterase Inhibitors with Photoswitchable Inhibition of β-Amyloid Aggregation. *ACS Chem. Neurosci.***2014**, 5, 377 – 389.

TOC